Nanotheranostics for Cancer: Integrating Imaging, Therapy, and Real-Time Monitoring

Trisha Manipatruni

ABSTRACT

Despite decades of progress, cancer is still often detected late, and treatment remains non-specific. Nanotheranostic platforms combine imaging and therapy into engineered nanoparticles and could enable earlier detection, precise intervention, and real-time monitoring of cancer. Nanotheranostic platforms incorporate novel light-activated treatments like phototherapy alongside standard treatments such as chemotherapy. In addition, nanotheranostics enable advanced magnetic resonance imaging (MRI) or fluorescence imaging, which allows real-time monitoring of treatment progress. By uniting diagnostics with therapeutics, these platforms aim to concentrate treatment at tumor sites, reduce systemic toxicity, enable real-time feedback, and ultimately improve treatment efficacy and patient quality of life. This review presents the various treatment, diagnostic, and targeting modalities of nanotheranostics to identify the most promising clinically translatable nanotheranostic strategies. Overall, many reports suggest combined therapeutic approaches integrating multiple therapeutic modalities perform best and are most likely to be clinically relevant.

Keywords: nanomaterials, cancer, nanotheranostics, theranostics

INTRODUCTION

Cancer continues to be a leading cause of death worldwide. In 2022, there were about 20 million new cases and nearly 10 million deaths globally [1]. By 2050, annual cases are projected to reach about 33 million, and the number of cancer-related deaths will rise to 18.2 million [1]. These trends reinforce the demand for earlier detection and more tumor-specific treatment strategies [2].

Current diagnostic tools have major drawbacks. Limited sensitivity and specificity can delay detection, which reduces treatment options and worsens outcomes [2,3]. Conventional imaging modalities such as computed tomography (CT) and magnetic resonance imaging (MRI) are essential for staging and treatment planning, yet sensitivity can be limited for very small lesions and microscopic disease. Confirmation of cancer still requires an invasive biopsy that samples only a small portion of the suspect tissue [3,5]. On the therapeutic side, chemotherapy and radiation therapy lack specificity and thus damage healthy tissues, causing severe side effects that limit the doses patients can tolerate [2,3]. Achieving tumor-targeted delivery is still a major challenge [3,6]. Although recent modalities such as immune checkpoint inhibitors, chimeric antigen receptor T-cell (CAR-T) therapy, gene-based approaches, and targeted agents (such as poly(ADP-ribose) polymerase (PARP) inhibitors) have improved outcomes in certain cancers, a

substantial proportion of patients either fail to respond, develop resistance, or experience considerable toxicity. Furthermore, delivery barriers and tumor heterogeneity continue to restrict the precision and efficacy of these therapies.

These diagnostic and therapeutic limitations have increased interest in nanotheranostic systems, which integrate sensitive imaging, targeted delivery, and treatment monitoring within a single platform. Nanotheranostics use single-particle platforms that integrate diagnosis, therapy, and response monitoring [2,3,7]. These engineered nanoparticles co-deliver a therapeutic payload and an imaging agent, while size and surface chemistry enable tumor accumulation and molecular targeting [3,8]. For example, a single carrier can deliver a chemotherapy drug and an MRI agent [8]. After targeting tumor cells and releasing the drug, the same nanoparticle enables imaging of the treatment response [8].

This review organizes nanotheranostic platforms into three domains: (i) therapy modalities, including photothermal therapy (PTT), in which light-absorbing agents convert near-infrared irradiation into localized heat; photodynamic therapy (PDT), where a photosensitizer generates cytotoxic reactive oxygen species upon light activation; conventional chemotherapy, which relies on cytotoxic drugs that disrupt cell proliferation; and combination platforms that integrate two or more of these treatments within a single construct. (ii) Diagnostic readouts, including magnetic resonance imaging (MRI), which provides deep-tissue anatomical and functional contrast, often enhanced by contrast agents, and fluorescence imaging, which uses emissive probes to visualize nanoparticle localization and, in some cases, report microenvironmental cues. (iii) Targeting strategies, including passive targeting via the enhanced permeability and retention (EPR) effect, where nanoparticles accumulate due to leaky tumor vasculature and poor lymphatic drainage; ligand-based active targeting, in which antibodies, peptides, aptamers, or small molecules bind overexpressed receptors to promote cellular uptake; and organelle targeting, where localization motifs direct payloads to compartments such as mitochondria, lysosomes, or nuclei to increase on-target damage. Building on this framework, the review examines design trade-offs for integrated systems that combine chemotherapy, phototherapy, and imaging within a single platform.

THERAPY

Four therapeutic modalities are examined in this review: photothermal therapy (PTT), photodynamic therapy (PDT), chemotherapy, and combination platforms. Each modality is described in terms of its core mechanisms and illustrated by a representative benchmark nanoplatform.

i. Phototherapy

Phototherapy uses light to induce a therapeutic effect (Figure 1). In photothermal therapy (PTT), near-infrared (NIR) light is absorbed and converted to localized heat that ablates tumor cells [2]. Heating can be preferentially localized to nanoparticle-enriched tissue exposed to near-infrared (NIR) light, which can reduce harm to untargeted cells [2]. PTT is functionally localized because photothermal agents are designed to accumulate in tumors more than normal tissue (EPR, active targeting), and clinicians restrict where the laser goes (focused beam, image guidance, or fiber delivery). For example, a graphene oxide–polymer hybrid heated from ~32 °C to ~64 °C within 5 minutes under 808 nm light killed about 80% of cancer cells in vitro [9]. The same platform also showed pH-responsive fluorescence, which is relevant because the tumor microenvironment is often mildly acidic, and intracellular trafficking after uptake places nanoparticles in acidic endosomes and lysosomes. A pH-activated signal can improve tumor-to-background contrast, help in outlining tumor margins, and support image-guided irradiation so that heating is applied when the agent is actually at the target site. Beyond carbon systems, diverse nanostructures support PTT. Reported PTT materials include gold nanorods, graphene-based composites, and carbon-nanotube variants [2,3]. PTT platforms can be constructed to simultaneously visualize and destroy tumors with heat while aiming to spare healthy tissues [2,10].

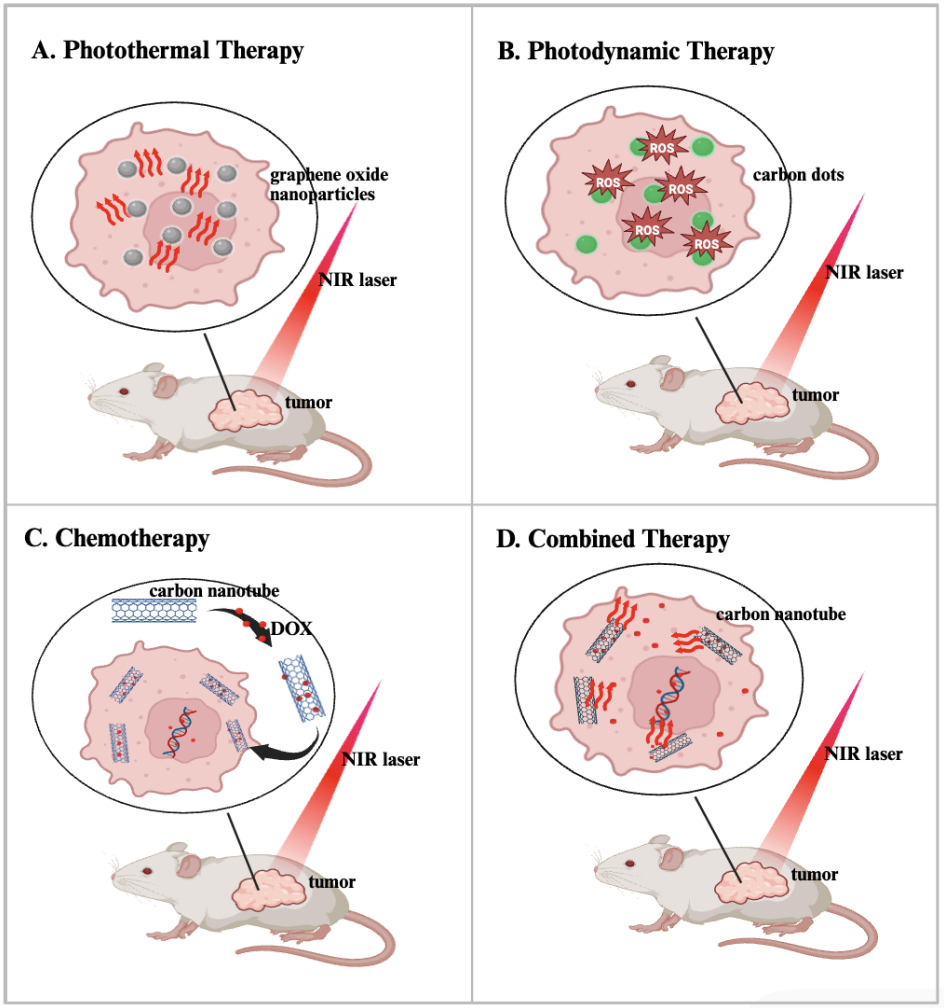

Figure 1. Nanotheranostic carbon platforms integrate imaging and therapy. (A) PTT: Nanoparticles accumulate in the tumor and, under NIR laser irradiation, generate localized heat for photothermal ablation. (B) PDT: Nanoparticles activated by visible or near-infrared light generate reactive oxygen species (ROS) inside tumor tissue, causing photodynamic cell death. (C) Carbon nanotubes carrying doxorubicin (DOX) enter tumor cells via endocytosis and release the drug. (D) Carbon nanotubes loaded with DOX release the drug upon irradiation while simultaneously generating heat for combined chemo-photothermal therapy.

ii. Photodynamic therapy (PDT)

In contrast to heat-driven ablation, photodynamic therapy (PDT) generates cytotoxic reactive oxygen species (ROS) upon light activation [11,12]. Nanotheranostic designs enhance PDT by coupling photosensitizers with targeting and imaging components [13,14]. For example, gold-nanostar aggregation-induced emission (AIE) nanodots provide bright fluorescence for imaging and efficient singlet-oxygen generation for PDT; in vitro, about 80% of cancer cells were killed within 10 minutes of light exposure, versus about 18% with the photosensitizer alone [13].

Hyaluronic-acid-derived carbon dots (HA-CDs) bind to CD44, a hyaluronic-acid receptor frequently overexpressed in many carcinomas and often used as a tumor-associated uptake marker. The HA–CD44 interaction enhances cellular internalization in CD44-high tumors and increases the selectivity of photodynamic therapy (PDT) compared to non-targeted uptake [14]. Under 650 nm irradiation, HA-CDs generate ROS and selectively reduce viability in CD44-high cells while providing fluorescence for imaging [14].

Incorporating manganese into HA-CDs, specifically by anchoring single-atom Mn on CDs, resulted in mitochondrial colocalization and enhanced ROS-mediated mitochondrial damage [15]. This finding is significant because mitochondria play a central role in redox regulation and apoptosis signaling. Therefore, generating ROS in close proximity to mitochondria can more effectively disrupt mitochondrial membrane potential and induce cell death compared to ROS generated at more distant cellular locations [15]. Organelle-proximal ROS delivery is particularly important in photodynamic therapy (PDT), as ROS are short-lived and have limited diffusion distances within cells.

Selenium/nitrogen co-doped carbon dots were reported to enable nuclear delivery and stronger PDT. This is mechanistically useful for the same diffusion reason: producing ROS at or inside the nucleus increases the chance of direct DNA damage and replication stress, which can drive rapid loss of viability [16]. In that system, the authors also describe RNA-associated localization and light-triggered nuclear entry, which helps explain why doped CDs showed near-complete in vitro cell death after a single light treatment, while undoped CDs did not localize to the nucleus and induced minimal cell death [16]. In a separate study, two-photon excitable carbon dots reduced HeLa viability to about 22% under 638 nm irradiation; in mice, intravenous dosing showed no obvious organ toxicity at 14 days, although antitumor efficacy was not evaluated [17].

Clinically, head and neck outcomes in early oral and laryngeal cancers largely reflect Photofrin-mediated PDT, typically using porfimer sodium dosing with a multi-hour drug–light

interval and red light around 630 nm delivered via optical fibers (for example, microlens or diffuser fibers) to illuminate the lesion while sparing surrounding structures [12,18].

iii. Chemotherapy

Chemotherapy remains a clinical workhorse for cancer care. Nanotheranostic platforms aim to improve efficacy by concentrating drugs in tumors and reducing systemic exposure [3]. One example is polyethylene glycol / polyethylenimine (PEG/PEI) functionalized single-walled carbon nanotubes (SWCNTs) loaded with doxorubicin (DOX) [19]. Mechanistically, polyethylene glycol (PEG) improves colloidal stability and prolongs circulation, while polyethylenimine (PEI) increases surface charge and can enhance cellular uptake. Many carriers also use pH-sensitive release because, after uptake, they encounter acidic endosomes and lysosomes, whereas blood and most normal tissues are closer to neutral pH.

Consistent with that design logic, these SWCNTs released >50% of DOX at pH 5.0 by 120 h, versus <40% at pH 7.4 [19]. Practically, this points to less premature drug leakage under physiological conditions and more release after cellular internalization. Flow cytometry also showed higher mean fluorescence at 12 h and 24 h compared with free DOX and other CNT carriers [19], which supports higher intracellular drug accumulation (not just “presence” in solution). Together, higher uptake plus acid-biased release helps explain why these carriers can increase tumor-cell kill while potentially lowering off-target exposure.

Multi-walled CNTs have also been used as DOX carriers with high loading (~270 mg/g) and faster release at pH 5.0 (further accelerated under NIR) [8]. In mice, combined chemo-photothermal therapy eradicated tumors without regrowth [8]. CQD polymer nanospheres similarly delivered DOX with pH- and NIR-triggered release [25]. In CNT composite platforms tested in mice, NIR-triggered chemo plus PTT produced stronger tumor control than DOX alone and showed acceptable safety [8]. By concentrating drugs within tumor cells and timing release to treatment, nanotheranostics can boost antitumor effects and may reduce systemic side effects relative to conventional chemotherapy [8,14,19].

iv. Combination Platforms

Combination platforms integrate two therapeutic modes (e.g., PTT plus chemotherapy) within one nanoparticle to boost tumor killing while lowering each component's dose [13,16,20]. For example, a PEGylated mesoporous silica-coated SWCNT (SWNT@MS-PEG) loaded with DOX forms an NIR-responsive system [21]: the SWCNT core is the NIR “heater,” the silica shell stores the drug, and the PEG coating improves stability and circulation.

Under 808 nm irradiation, local temperatures rise (to ~48 °C in tumors), enabling photothermal damage, enhancing cellular uptake, and promoting intracellular drug release [21]. This system was tested on cancer (4T1, HeLa) and non-cancer (293T) cell lines. Combined chemo-photothermal treatment killed more cancer cells than either mode alone, consistent with PTT enhancing drug effectiveness by improving delivery and release.

In representative studies, dual-function designs improve cell killing in vitro and, in mice, suppress tumors more effectively than chemotherapy or PTT alone [8,21]. Adding imaging to these carriers makes treatment more controllable. For example, incorporating a T1-weighted MRI contrast component and a fluorescent label into the same carrier can enable confirmation of tumor accumulation before irradiation and support image-guided therapy. Verifying agent location before irradiation allows better timing and localization, reduces off-target effects, and improves reproducibility.

DIAGNOSTICS/IMAGING

Fluorescence imaging offers high sensitivity and cellular-level resolution. Many platforms intrinsically fluoresce or carry fluorescent tags for tumor visualization [10,20]. Copper-doped carbon dots (Cu-CDs) achieved a fluorescence quantum yield of ~24% and a singlet-oxygen yield of ~36%, enabling clear imaging of cancer cells and 3D tumor spheroids while driving PDT to inhibit spheroid growth under light [20]. Some nanoparticles extend emission after excitation through afterglow luminescence. The nanoparticles reduce background noise from autofluorescence, providing improved signal-to-noise ratios for imaging tumors.

Near-infrared afterglow aggregation-induced emission (AIE) dots co-loaded with TPE-Ph-DCM and a Schaap's dioxetane precursor in a lipid-PEG matrix can emit persistently after brief pre-irradiation [22]. Reported afterglow lasts >10 days in buffer and has an ~48-min half-life in blood [22]. In mice, afterglow imaging yielded ~100× higher tumor-to-liver contrast than conventional fluorescence and enabled image-guided surgery [22]. The key advantage is that the signal is collected after excitation is off, which suppresses tissue autofluorescence and boosts tumor-to-background contrast.

Multimodal fluorescent nanoparticles such as red-emissive CDs offer both strong fluorescence and photoacoustic signals (ultrasound waves generated when tissue absorbs pulsed light) for dual-mode imaging with photothermal treatment [10]. Fluorescent nanotheranostics can also be engineered to respond to tumor-specific triggers such as acidic pH. Solid tumors and intracellular trafficking compartments are often more acidic than blood, so pH-activated ("turn-on") probes can stay dim during circulation and brighten after tumor uptake, improving tumor-to-background contrast. For example, a pH-responsive graphene oxide hybrid remains quenched at physiological pH but fluoresces strongly in acidic conditions typical of tumors,

enabling tumor-selective imaging alongside photothermal therapy [9]. Integrating imaging with therapy allows real-time monitoring, confirming nanoparticle accumulation, verifying light delivery, and tracking response over time [8,14,21,23].

TARGETING

Targeting is a third component of nanotheranostics: selective tumor accumulation enables potent therapy and high-contrast imaging (Figure 2)

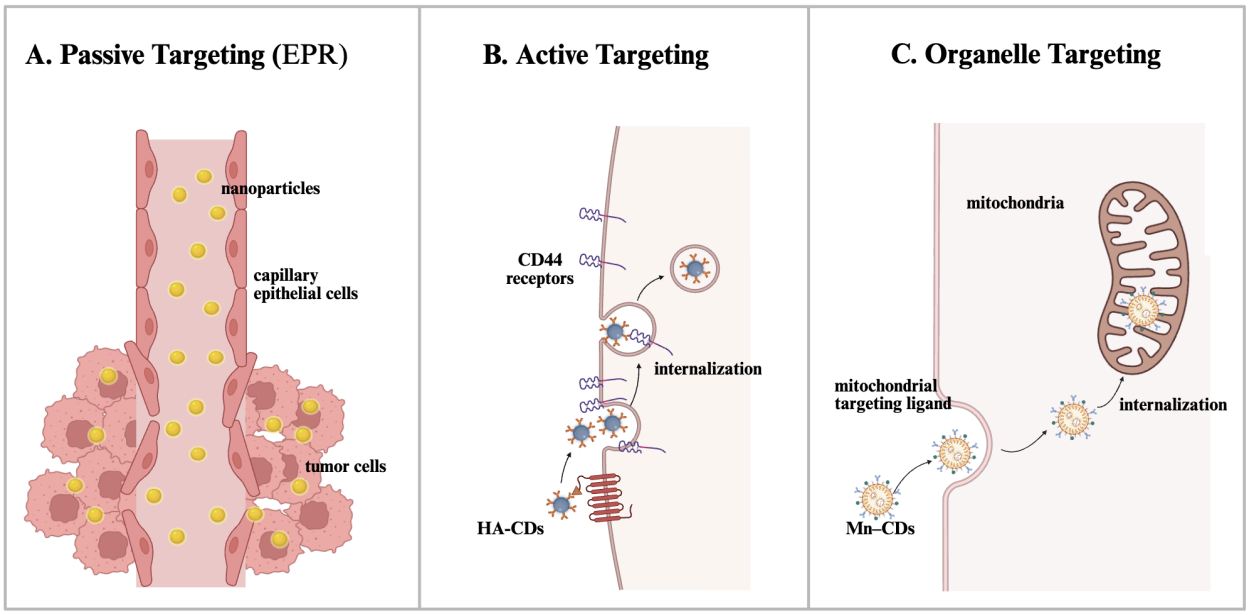

Figure 2. (a) Nanoparticles circulate in blood and passively accumulate in tumors because tumor vasculature is irregular and leaky (enhanced permeability and retention (EPR) effect), and particles are retained due to poor lymphatic drainage. (b) Surface ligands (e.g., hyaluronic acid) bind receptors such as CD44 on tumor cells, promoting receptor-mediated endocytosis and payload release. (c) Nanoparticles tagged with mitochondrial-targeting ligands enter tumor cells and concentrate in mitochondria, releasing payloads directly within the organelle.

Passive Targeting

Passive targeting exploits the enhanced permeability and retention (EPR) effect: particles tens-to-hundreds of nanometers in size extravasate through aberrant tumor vasculature and are retained more than in normal tissue. PEGylation extends circulation half-life by reducing immune clearance, which can enhance EPR-mediated uptake. In vivo CNT composites increased tumor uptake and apoptosis versus controls [8]. SWNT–PEG–PEI increased cellular uptake and

accelerated DOX release at pH 5.0 in MCF-7 cells [19]. Taken together, these results support the basic passive-targeting logic: longer blood residence plus tumor leakiness increases the chance particles accumulate in tumors, and once internalized, acidic compartments promote drug release, which can raise apoptosis in tumor cells while limiting exposure in normal tissues.

Active Targeting

Active targeting uses surface ligands such as antibodies, peptides, and small molecules that bind tumor-associated receptors. Under 650 nm light, hyaluronic-acid–modified carbon dots (HA-CDs) bind CD44 and cut cancer cell viability to ~20–30% while sparing normal cells in vitro [14]. Anti-epidermal growth factor receptor (EGFR) antibody functionalization further improved uptake and increased cytotoxicity compared with non-targeted carriers [8]. In another active-targeting approach, hyaluronic acid can cap mesoporous silica nanoparticles, improving tumor-cell interactions via HA-recognition while enabling bioresponsive uncapping and drug release in relevant biological environments [24]. Folate-mediated active targeting is widely used because folate receptor-α is overexpressed in several tumor types and can promote receptor-mediated endocytosis when nanoparticles are decorated with folic acid. Folate-functionalized carbon quantum dots have been reported to increase uptake in folate-receptor-positive cells and improve doxorubicin (DOX) delivery, including pH-responsive release, relative to free drug [25].

Organelle targeting

Nanoparticles can also be functionalized with organelle-targeting ligands to increase efficacy by placing the payload near vulnerable intracellular structures (e.g., mitochondria or the nucleus). Organelle targeting can also increase efficacy by placing ROS generation near vulnerable intracellular structures. For example, single-atom Mn anchored on carbon dots increased mitochondrial colocalization and enhanced ROS-mediated mitochondrial damage [15]. Nuclear-proximal ROS generation has also been used to intensify PDT by placing oxidative stress closer to DNA [16].

Combining passive accumulation with molecular and organelle-level targeting can increase tumor specificity. Enhanced targeting concentrates payloads in cancer cells and specific organelles, improves imaging contrast, and may enable more effective, safer treatment paradigms [3,11,14].

Overall, passive targeting increases the odds of tumor accumulation through pharmacokinetics, active targeting increases cellular uptake through receptor binding, and organelle targeting increases potency by placing the payload where it can do the most damage with minimal diffusion loss.

CONCLUSION

This review surveyed nanotheranostic platforms across major therapy modalities (PTT, PDT, chemotherapy, and combination approaches), paired with imaging readouts (most commonly fluorescence and MRI) and targeting strategies (passive EPR, ligand-based active, and organelle targeting). Across platforms, the practical value of integration is straightforward: imaging verifies where the agent is, therapy is activated locally (often by light), and follow-up imaging can track whether the tumor is responding. The recurring design challenge is balancing multifunctionality with simplicity, since each added component can increase off-target interactions and complicate scale-up.

Translating nanotheranostics to clinical practice requires progress on several fronts. Few nanoparticle platforms have reached clinical trials. Reported hurdles include immunotoxicity and less-than-ideal tumor accumulation in humans [2,6]. Long-term safety, low immunogenicity, and scalable manufacturing are critical requirements [2,6]. Promising strategies include using materials with favorable biodegradation and clearance profiles, and improving active targeting to raise intratumoral uptake [2,6] (Table 1).

Biocompatibility depends strongly on material composition, purity, and surface chemistry. Residual catalysts and other impurities can increase oxidative stress and confound toxicity results, so rigorous purification and thorough physicochemical characterization are essential [2,6].

Platforms built on clinically tested components are attractive because of known biocompatibility. Several photothermal and liposomal candidates have entered clinical evaluation [2]. Single-modality treatments rarely eradicate tumors; the most effective path couples synergistic therapies (e.g., chemo-plus-photo) with integrated diagnostics [2,8,21,22].

Multimodal, targeted nanotheranostics could improve outcomes by enabling earlier detection, precise delivery, and real-time response monitoring. Focusing research on translational hurdles and the most viable platforms can accelerate progress toward personalized, adaptive cancer therapy [2,3].

SUMMARY OF NANOPLATFORMS

Table 1. Summary of preclinical nanoplatforms for cancer therapy and imaging, reporting material, therapy modality, imaging modality, targeting strategy, model system, dosing or irradiation conditions, outcome metrics, key strengths, and source.

Nanoplatform	Therapy modality	Imaging modality	Targeting strategy	Model	Outcome	Source
SWNT–PEG (DSPE–mPEG–coated single-walled carbon nanotubes; NIR-II fluorophores)	—	NIR-II fluorescence (1.0–1.4 μm)	Passive (circulation/EPR)	In vivo: mice (IV [a])	• Time-resolved organ dynamics: lung contrast peak at ~3.5 s post-injection; kidney contrast peak at ~5.2 s; steady-state by ~15 s (one-pass circulation). • Depth advantage vs NIR-I: tissue-phantom experiments show slower loss of feature contrast with depth in NIR-II than NIR-I.	[4]

SWNT–RGD (PL-PEG5k–SWNT + cyclic RGD)	—	Photoacoustic (690 nm)	Active (αvβ3)	In vivo: U87MG [b] xenografts, mice (IV)	• ~8× higher tumor PA signal vs non-targeted SWNTs. • 3D PA/US maps targeted SWNTs in tumors up to 4 h post-injection.	[5]
SWNT–DOX (branched-PEG–functionalized single-walled carbon nanotubes with π–π–stacked doxorubicin)	Chemotherapy (nanocarrier)	—	Passive (EPR via prolonged circulation)	In vivo: mice, Raji [c] lymphoma xenografts (IV)	• ~10× longer t½ (0.21→2.22 h) and ~2× higher tumor DOX (0.68→1.51 %ID/g). • Stronger tumor inhibition than free DOX at 5 mg/kg. • Low toxicity: minimal weight loss	[7]
MWCNT–GdN@CQDs/DOX–EGFR	Combination (PTT + chemo)	FL + MRI	Active (EGFR)	In vivo (mice; 808 nm)	• Peak tumor temp ~52 °C under 808 nm irradiation. • complete tumor regression with no relapse at 14 days. • pH/NIR-triggered DOX release augments the PTT effect	[8]

rGO/[PEDOT:D-PSM]:C/B-PgP (reduced graphene oxide hybridized with an ionic PEDOT complex and a catechol-BODIPY PEG copolymer)	PTT (808 nm)	Fluorescence (pH-responsive)	—	In vitro: KB d & MDA-MB-231 cells	• Efficient NIR heating under 808 nm (IR camera readouts; concentration-dependent temperature rise). • Cell uptake visualized by confocal microscopy; photothermal cytotoxicity by MTT. • pH-tunable fluorescence for imaging in acidic environments.	[9]
Red-emissive carbon dots (PPA-derived C-dots)	PTT (thermal)	FL + PA	Passive	SubQ [f] (HeLa xenograft in mice	• Photothermal conversion efficiency 38.5% at 671 nm. • NIR irradiation produced tumor temperature elevations sufficient for ablation and significant regression in living mice	[10]

HA-derived carbon dots (HA-CDs)	PDT (650 nm)	Fluorescence	Active (HA–CD44)	In vitro	• CD44-high cells reduced to ~20–30% viability after light exposure, indicating selective • ROS-mediated killing vs low-CD44 controls.	[14]
Se/N-doped carbon dots (Se/N-CDs)	PDT (nucleus-proximal ROS)	Fluorescence	RNA-assisted nuclear entry	In vitro HeLa [9] + mouse safety	• DNA-proximal ROS yields marked cell-kill in vitro. • in-vitro kill plus in-vivo tumor-growth inhibition reported;	[16]
Two-photon red CDs (TP-CDs)	PDT (two-photon excited)	Two-photon FL (~605 nm)	Nucleolus-targeting (RNA affinity)	In vitro (HeLa)	• Post-irradiation cell viability ≈ 22%, showing strong nucleolus-targeted PDT. • no organ toxicity at 14 days reported in mouse safety check (efficacy not tested in vivo).	[17]

Photofrin-based PDT (early oral & laryngeal)	PDT (630 nm)	—	—	Clinical (n = 276)	• Complete response after one treatment: 94% (oral) and 91% (laryngeal); with salvage therapy, • ~100% long-term control while preserving speech/swallowing in most patients.	[18]
PEG/PEI-functionalized SWCNTs (SWNT–PEG–PEI) loaded with DOX	Chemo (nanocarrier)	—	Passive (EPR; uptake ↑ by PEI)	In vitro MCF-7[h]	• Higher cellular uptake vs carboxylated/PEG-only CNTs. • faster DOX release at pH 5.0; enhanced cytotoxicity to MCF-7.	[19]
Cu-doped carbon dots (Cu-CDs)	PDT	Fluorescence	Passive	In vitro HeLa + 3D spheroids	• $1O_2$ quantum yield ≈36%; HeLa/3D spheroid growth strongly inhibited after light exposure.	[20]
SWNT@MS-PEG/DOX (mesoporous-silica–coated SWNTs,	Combination (NIR PTT + chemo)	PA + MR	Passive (EPR)	In vivo: tumor-bearing mice (IV; 808 nm)	• On-demand DOX release under NIR; tumor temperature	[21]

PEGylated, DOX-loaded)					~48 °C at 808 nm. • PA/MR verify efficient tumor accumulation. • PTT+ chemo achieves stronger tumor suppression than either monotherapy at low drug/laser dose.	
AGL AIE dots (near-IR afterglow AIE nanoparticles)	(image-guided surgery)	NIR afterglow	Passive (EPR)	Peritoneal tumors; carcinomatosis model)	• Tumor-to-liver signal ratio ~100× (afterglow vs fluorescence), enabling precise resection of many small peritoneal nodules.	[22]

[a] IV indicates intravenous administration.

[b] U87MG denotes a human glioblastoma cell line xenograft in mice.

[c] Raji denotes a human B-cell lymphoma xenograft in mice.

[d] KB denotes a human oral epidermoid carcinoma cell line (in vitro).

[e] MDA-MB-231 denotes a human triple-negative breast cancer cell line (in vitro).

[f] SubQ indicates a subcutaneous flank xenograft in mice.

[g] HeLa denotes a human cervical cancer cell line/xenograft.

[h] MCF-7 denotes a human ER-positive breast adenocarcinoma cell line (in vitro)

ABBREVIATIONS

Abbreviation	Definition
AIE	Aggregation-induced emission
CAR-T	Chimeric antigen receptor T-cell
CDs	Carbon dots
CNT	Carbon nanotube(s)
CT	Computed tomography
DOX	Doxorubicin
DSPE–mPEG	1,2-Distearoyl-sn-glycero-3-phosphoethanolamine–methoxy(polyethylene glycol)
EPR	Enhanced permeability and retention
EGFR	Epidermal growth factor receptor
FL	Fluorescence
Gd	Gadolinium
HA	Hyaluronic acid
H2O2	Hydrogen peroxide
ID/g	Injected dose per gram (typically reported as %ID/g)
IV	Intravenous
mPEG	Methoxy polyethylene glycol
MR	Magnetic resonance
MRI	Magnetic resonance imaging
MTT	3-(4,5-Dimethylthiazol-2-yl)-2,5-diphenyltetrazolium bromide (MTT assay)
MWCNT	Multi-walled carbon nanotube(s)
NIR	Near-infrared

Abbreviation	Definition
NIR-I	First near-infrared window
NIR-II	Second near-infrared window
PA	Photoacoustic
PARP	Poly(ADP-ribose) polymerase
PDT	Photodynamic therapy
PEG	Polyethylene glycol
PEI	Polyethylenimine
PEDOT	Poly(3,4-ethylenedioxythiophene)
PL–PEG	Phospholipid–polyethylene glycol (lipid–PEG)
PTT	Photothermal therapy
QY	Quantum yield
RGD	Arg-Gly-Asp peptide (integrin-binding motif)
rGO	Reduced graphene oxide
ROS	Reactive oxygen species
SubQ	Subcutaneous
SWCNT	Single-walled carbon nanotube(s)
SWNT	Single-walled nanotube(s)
t½	Half-life
T1	T1-weighted (as in T1-weighted MRI)
TAT	Trans-activator of transcription (TAT) peptide (cell-penetrating peptide)
TPE-Ph-DCM	AIE fluorophore (as named in the cited study; tetraphenylethene-based dye)
TPP	Triphenylphosphonium (mitochondria-targeting cation)
UCNP	Upconversion nanoparticle(s)

Abbreviation	Definition
US	Ultrasound
%ID/g	Percent injected dose per gram
$^1O2$	Singlet oxygen

Note: “SWNT” and “SWCNT” refer to the same class of materials

REFERENCES

1. Bray, F., Laversanne, M., Sung, H., Ferlay, J., Siegel, R. L., Soerjomataram, I., & Jemal, A. Global cancer statistics 2022: GLOBOCAN estimates of incidence and mortality worldwide for 36 cancers in 185 countries. CA: A Cancer Journal for Clinicians. 2024;74(3):229–263. Accessed June 27, 2024. https://pubmed.ncbi.nlm.nih.gov/38572751/
2. Gai S, Yang G, Yang P, He F, Lin J, Jin D, et al. Recent advances in functional nanomaterials for light-triggered cancer therapy. Nano Today. 2018;19:146–187.
3. Dai L, Qu Y, Yang S. Carbon nanomaterials for biological imaging and nanomedicinal therapy. Chem Soc Rev. 2015;44(14):6023–6057.
4. Welsher K, Sherlock SP, Dai HJ. Deep-tissue anatomical imaging of mice using carbon nanotube fluorophores in the second near-infrared window. Proc Natl Acad Sci U S A. 2011;108:8943–8948.
5. De La Zerda A, Zavaleta C, Keren S, Vaithilingam S, Bodapati S, Liu Z, et al. Carbon nanotubes as photoacoustic molecular imaging agents in living mice. Nat Nanotechnol. 2008;3:557–562.
6. Chen Z, Wang Z, Gu Z. Bioinspired and biomimetic nanomedicines. Acc Chem Res. 2019;52(5):1255–1264.
7. Liu Z, Fan AC, Rakhra K, Sherlock S, Goodwin A, Chen XY, et al. Supramolecular stacking of doxorubicin on carbon nanotubes for in vivo cancer therapy. Angew Chem Int Ed. 2009;48:7668–7672.
8. Zhang M, Wang W, Wu F, Yuan P, Chi C, Zhou N, et al. Magnetic and fluorescent carbon nanotubes for dual-modal imaging and photothermal and chemo-therapy of cancer cells in living mice. Carbon. 2017;123:70–83.
9. Sharker SM, Kang EB, Shin C-I, et al. NIR-active, pH-responsive rGO hybrid for imaging-guided PTT. J Appl Polym Sci. 2016;133:43791.
10. Ge J, Jia Q, Liu W, Guo L, Liu Q, Lan M, et al. Red-emissive carbon dots for fluorescent, photoacoustic, and thermal theranostics in living mice. Adv Mater. 2015;27:4169–4177.
11. Fan W, Huang P, Chen X. Overcoming the Achilles’ heel of photodynamic therapy. Chem Soc Rev. 2016;45:6488–6519.
12. Agostinis P, et al. Photodynamic therapy of cancer: An update. CA Cancer J Clin. 2011;61(4):250–281.

13. Yaraki MT, Wu M, Middha E, et al. Gold nanostars–AIE theranostic nanodots for image-guided PDT. Nano-Micro Lett. 2021;13:58.
14. Zhang L, Lin Z, Yu Y-X, Jiang B-P, Shen X-C. Hyaluronic-acid-derived carbon dots for self-targeted imaging-guided PDT. J Mater Chem B. 2018;6:6534–6543.
15. Wang S, Ma M, Liang Q, Wu X, Abbas K, Zhu J, et al. Single-atom manganese anchored on carbon dots for promoting mitochondrial targeting and photodynamic effect in cancer treatment. ACS Appl Nano Mater. 2022;5:6679–6690.
16. Xu N, Du J, Yao Q, et al. Se/N-doped carbon dots for precise PDT via nuclear envelope penetration. Carbon. 2020;159:74–82.
17. Yi S, Deng S, Guo X, et al. Red-emissive two-photon CDs for nucleolus-targeted PDT with real-time monitoring. Carbon. 2021;182:155–166.
18. Biel MA. Photodynamic therapy treatment of early oral and laryngeal cancers. Photochem Photobiol. 2007;83(5):1063–1068.
19. Yang S, Wang Z, Ping Y, et al. PEG/PEI-functionalized SWCNTs as DOX carriers: Loading/release/uptake. Beilstein J Nanotechnol. 2020;11:1728–1741.
20. Wang J, Xu M, Wang D, et al. Copper-doped carbon dots for optical bioimaging and photodynamic therapy. Inorg Chem. 2019;58:13394–13402.
21. Liu J, Wang C, Wang X, et al. Mesoporous silica-coated SWNTs for imaging-guided combination therapy. Adv Funct Mater. 2015;25:384–392.
22. Ni X, Zhang X, Duan X, et al. NIR afterglow AIE dots with ultrahigh tumor-to-liver ratio for image-guided surgery. Nano Lett. 2019;19:318–330.
23. Jia Q, Ge J, Liu W, Zheng X, Chen S, Wen Y, et al. A magnetofluorescent carbon dot assembly as an acidic H2O2-driven oxygenator to regulate tumor hypoxia for simultaneous bimodal imaging and enhanced photodynamic therapy. Adv Mater. 2018;30:1706090.
24. Chen Z, Li Z, Lin Y, Yin M, Ren J, Qu X. Bioresponsive hyaluronic acid-capped mesoporous silica nanoparticles for targeted drug delivery. Chem Eur J. 2013;19:1778–1783.
25. Chiu SH, Gedda G, Girma WM, Chen JK, Ling YC, Ghule AV, et al. Rapid fabrication of carbon quantum dots as multifunctional nanovehicles for dual-modal targeted imaging and chemotherapy. Acta Biomater. 2016;46:151–164.